Robot-Assisted Detection and Stiffness Prediction of Breast Tumor

Yun-Chi Hsieh, Dar-Ren Chen, Ruei-Hao Fan, Yu-Che Liu, and Ping-Lang Yen*

***Abstract*—A methodology of robot-assisted breast tumor detection and stiffness prediction has been established. In the paper, a statistical shape model for tumor morphology was built and utilized for tumor phantom fabrication in palpation experiments. The force signals acquired from robot-held probe during the automated palpation were pre-processed to reduce the surrounding tissue effect before the subsequent detection of force peak, slope feature, and shape correlation. The tumor detection by the proposed algorithm could produce robust results for tumor existence. Subsequently the force curve features were also extracted for training the Support Vector Regression (SVR) model for tumor stiffness prediction. The result showed that the prediction error was 8% and 15% respectively for the trained and interpolated stiffness for the testing set. The accuracy of stiffness prediction is acceptable for providing the second opinion as a companion to image modality for breast cancer diagnosis.**

***Index Terms*— Robot-Assisted Diagnosis, Biomechanics, Breast Cancer**

I. Introduction

In accordance with WHO's (World Health Organization) statistics, cancer deprived 8.2 million people of their lives in 2012 [1]. Among of various kinds of cancers, Breast Cancer was the most frequent types for women. Lack of timely diagnosis led to curative treatments become useless [2]. As a result, immediate researches about breast cancer to provide timely diagnosis and treatment are necessary. Nowadays, ultrasound is often used on breast tumor examination because of three merits: easy to distinguish cyst from tumor, no radiation and low-cost [3]. Nevertheless, it also has drawbacks. For example, ultrasonic images are blurry due to the shadow generated by echo. To improve accuracy, additional biopsy procedures must be carried out, which are invasive and reduce patients' desire to receive such checkup [4]. Thus, investment in breast cancer diagnosis is necessary.

Physical examination, though subjective, is common now to find breast tumor: patients describe their symptoms while physicians check irregular parts by palpation [5]. If we can determine if there exist a tumor and quantify biomechanical property between different tumors, it will definitely bring great benefits in breast tumor diagnosis [6-7]. In this research, we analyzed force relation between probe and tumor, determine the existence of tumor, position it and then created a model based on stiffness ratio between tumor and tissue. Integrating this stiffness prediction model with ultrasound image, this system can provide addition-al information for physician improving breast cancer diagnosis accuracy.

Biomechanical analysis on tissue is extremely intricate because of the deformation when palpating [8-9]. In other words, it's hard to derive an equation of static equilibrium between the stress and tumor. Hence, the analysis of tumor stiffness must be not on the basis of the equation but statistics. That is, the system makes prediction on some kinds of data which describes the stiffness of tumors. On the other hand, there are abundant information related to tumor's stiffness such as size, shape or position, there is a need to determine whether it is important or not in tumor's stiffness prediction. With previous demands, a palpation robot solution has been proposed to achieve the goal. Robot-automated platform offers the stable palpation properties of the phantom tumor [10]. With the force information measured, the detection of tumor position can be more precise and finished in few minutes. In following section, the paper will describe the robot-assisted palpation system for tumor examination in four parts. First, because it is nearly impossible to fabricate all kinds of tumor phantoms which were used in the experiments afterward, decisive factors for tumor phantom model were designed. Second, a robotic arm as well as a load cell was chosen to detect the stiffness of phantoms, simulating palpation in reality. Third, a tumor detection scheme was proposed to locate the tumor. In the end, enter the data of tumor phantoms that its stiffness ratio we have already known into our biomechanical model, and then the model can predict unknown samples.

II. Method

A palpation robot for automated breast tumor exploration is proposed as Fig. 1. The robot is equipped with a palpation probe on a force sensor, which is attached to the end-effector. The force sensor is able to measure the contact forces on the palpation probe as the probe touches the soft tissue surface during palpation procedure. The palpation contact forces are related to the indentation depth and moving speed of the probe, relative distance to the tumor, stiffness of the soft tissue and tumor and tumor morphology etc. The complex relationship could be described as the equation as Eq. (1) of which the analytic solution does not exist. However experimental approach together with a large amount of data could provide a good solution for finding the solution of the inverse problem of Eq. (1).

This paper was submitted on December 20, 2021.

This work was supported in part by the Ministry of Science and Technology, Taiwan under grant no. MOST 104-2221-E-002 -090 -MY2.

Yun-Chi Hsieh, Ruei-Hao Fan and Yu-Che Liu are with Department of Biomechatronics Engineering, National Taiwan University, Taipei, Taiwan.

Dar-Ren Chen is with Department of Surgery, Changhua Christian Hospital, ChangHua, Taiwan

Ping-Lang Yen is with Department of Biomechatronics Engineering, National Taiwan University, Taipei, Taiwan (e-mail: plyen@ntu.edu.tw), The corresponding author.

$$f = \boldsymbol{g}(a, d, x, \boldsymbol{s}, k) \quad (1)$$

where f is the measured force from the probe, a is the geometric parameter of the probe, d is the indentation depth, x is the probe position relative to the tumor, s the morphology of the inclusion, and k is the stiffness ratio of the inclusion to the surrounding tissue. For the experimental approach, the forward problem is to build the data set relating the contact forces with all the parameters of the probe geometry a, indentation depth d, position relative to the tumor x, morphology of the inclusion, and tumor stiffness relative to the surrounding tissue k. Then the tumor stiffness ratio is trying to find by solving the inverse problem using machine learning algorithm.

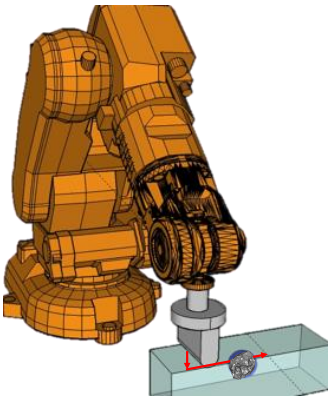

Fig. 1. Robot-Assisted Palpation for Breast Tumor Examination

A. *Reconstruction of tumor's shape*

First of all, breast phantoms with tumors were prepared for robot assisted palpation experiments. These phantoms were fabricated with reference to the 3D breast ultrasonic images from 259 human subjects scanned by a 3D ultrasound machine (Voluson 730, GE Healthcare, USA). Among these breast tumors were 145 benign and 115 malignant individually. The 4D view software of the ultrasound machine also provides image enhancement, segmentation and 3D reconstruction function to output the 3D model of the segmented tumor. The 3D reconstruction process of the tumors is shown in Fig. 2. The output is a STL format of 3D surface model with down-sampling to 1272 triangular facets.

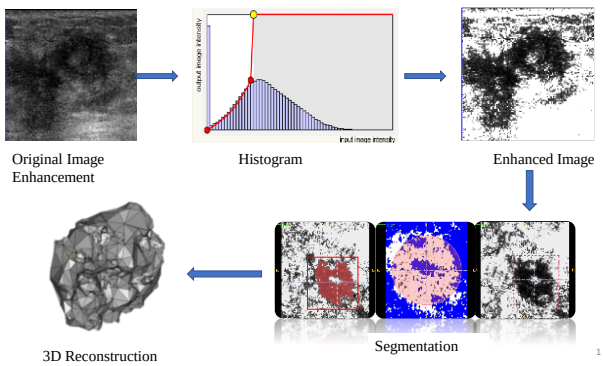

Fig. 2 The 3D reconstructed Breast Tumor from Ultrasound Imaging

Then the point distribution model [11] was applied to construct the mesh on the surface of tumors and presents each tumor as a vector. As shown in Fig. 3, first, alignment of the tumors is performed. Center of centroid of each tumor is assigned to the origin, and long axis of the tumor as the X-axis, short axis on the circumference of cross section, which contains origin and is perpendicular to X-axis, as the Y-axis. Then a unit sphere is constructed to project an arrow to find the intersection point with the facet of the tumor. These intersected points are then used to represent the morphology features of the tumors.

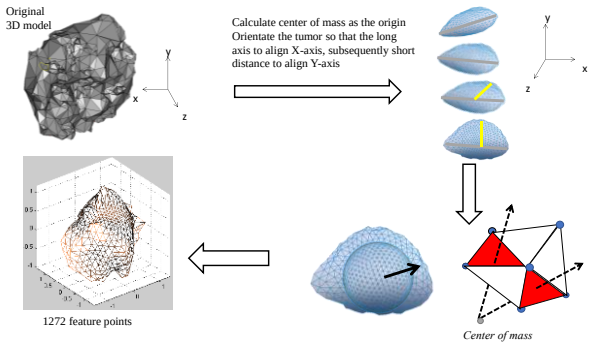

Fig. 3 Vector Representation of Tumor Morphology

Therefore each tumor's 3D geometry (after normalization) will be represented by a column vector of dimension 3816 (i.e. 1272 points in x, y and z coordinates).

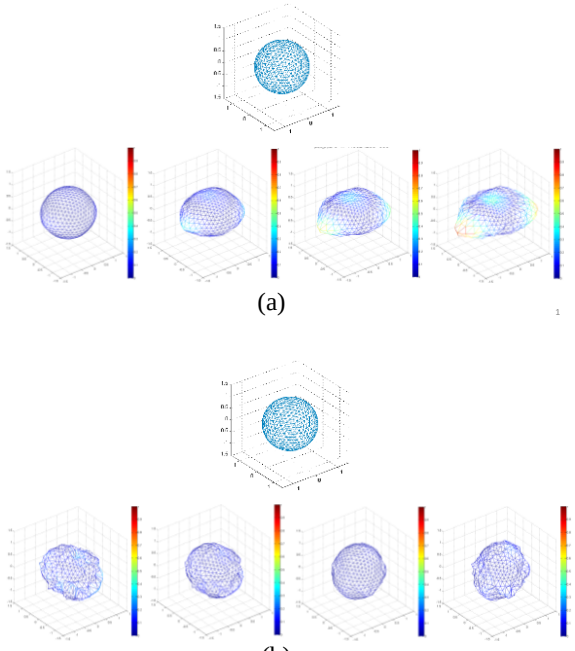

Fig. 4 Statistical Shape Model of the Tumor (a) The First Component, (b) The Second Component

However, the raw data's dimension is huge, useful data has to be determined and the data set are then simplified because it is impossible to fabricate all kinds of tumors. Tumors' shapes are irregular and involved many details, however which have little impact on biomechanical forces during palpation. The

dimension reduction can be effectively fulfilled by using PCA (principal component analysis) method. The first and second principal components were chosen to adequately represents tumor shape on them in biomechanics aspect. As shown in Fig. 4, the first and second components of the statistical shape model represents the tumor's outlooks and details.

Therefore the morphology factors (two components with 5 coefficients: -2σ, $-\sigma$, 0, σ, 2σ, where σ is the standard deviation), size (6mm, 9mm, 12mm, 15mm), stiffness ratio to surrounding tissue (5, 10, 15) are chosen to fabricate the tumor phantoms [12] as shown in Fig. 5.

Fig. 5 The Fabricated Tumor Phantom Modules

B. Computer Assisted Tumor Detection and Stiffness Prediction

An industrial robot arm (IRB-140, ABB Inc., Sweden) was equipped with a palpation probe with a load cell (LM-100N, Jihsense Inc., Taiwan) in between as shown in Fig. 6. The palpation probe with smooth and semicircular indentation side which is 10mm width and 40mm thick is mounted to the end-effector of the ABB robot arm.

Fig. 6 The ABB Robot Equipped with Force Sensor and Palpation Probe

Error! Reference source not found. shows that the robot was commanded to palpate a phantom with an embedded inclusion inside by moving along a predefined path, and at the same time, the resistant force versus the moving distance were recorded. The probe moved in constant velocity 5mm/s and the load cell measured forces that were orthogonal to the direction of movement. The silicon phantoms are soft, so we define the contact point when the voltage measured is 10mV higher than no load to avoid height errors. The data were utilized for two purposes. One is to study whether an underlying inclusion could be detected, and subsequently, the other is to determine the stiffness of the inclusion.

A typical measured force curve is shown in **Error! Reference source not found.**ig. 7. Signal processing and feature extraction for the measured data are necessary. The process is proceeded as follows:

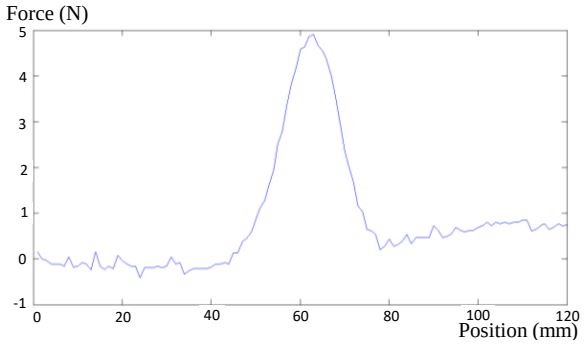

Fig. 7 The Measured Contact Forces During Palpating the Tumor

(1) Elimination of the background force

A background force related to pushing the surrounding tissue is subtracted from the measured force so that the force only reflects the pushing force to the tumor. After subtraction, the force signal displayed an increasing to the peak value then decreasing signal after passing through the tumor as shown in Fig. 8.

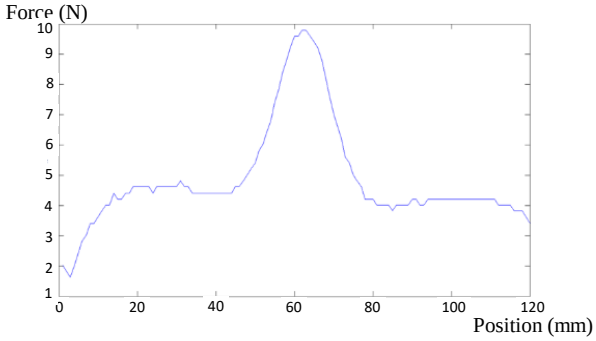

Fig. 8 A Typical Contact Force Curve When the Probe Passing over the Tumor

(2) Examination the peak value and slope property

If the peak value in the force curve is higher than the preset threshold value, there is a potential of tumor existence at the location. A subsequent calculation of slope property will be followed. The slope property at this location will be examined to reduce the false positive possibility for tumor existence. The slope property is obtained by differentiating the force curve with step size of 3mm. Then the obtained slope will be checked whether processes the feature of a positive value followed by a negative one (as the red dots shown in Fig. 9) corresponding to the movement of the probe passing through a tumor.

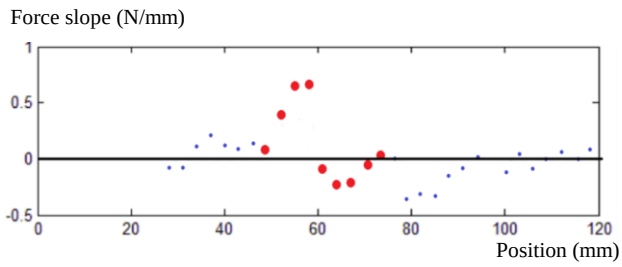

Fig. 9 The Slope Property of the Force Curve When Passing over a Tumor

(3) Shape correlation of the force curve shape

The correlation formula in Eq. (2) is further used to confirm the shape similarity of the measured force curve and the nominal one such as shown in Fig. 8.

$$r = \frac{\Sigma(f_i - \bar{f})(f_{0,i} - \bar{f}_0)}{\sqrt{\Sigma(f_i - \bar{f})^2}\sqrt{\Sigma(f_{0,i} - \bar{f}_0)^2}} \quad (2)$$

where f_i and $f_{o,i}$ are the measured and nominal force curve respectively; $\bar{f}$ and $\bar{f}_0$ are the mean values of the measured and nominal forces respectively. If the correlation r at the potential location of tumor existence is larger than a threshold value, then the tumor existence is finally confirmed. In summary, tumor detection algorithm will firstly locate where the force peaks arise from the measured force data. Then both the force slope property and shape correlation of the force curves will be further checked at these locations. If both features are satisfied, the screening outcome will confirm the existence of tumors at these locations.

C. Tumor stiffness prediction

The force curve, at the same time, is utilized for tumor stiffness prediction. The force data curves (force versus position) from the training sets were utilized to extract the features by PCA. The first 5 principal components held 99.8% descriptive level and could effectively represent the force curve features. All the samples are separated into training set (with 305 samples) and testing set (with 18 samples). Then the SVR model has been proposed to find the stiffness ratio of the tumor [13-14]. SVR with Radius Basis Function (RBF) kernel has the advantages of fitting the small amount of experiment data to the high nonlinear complex relationships between the tumor stiffness and the features of force data, palpation parameters and tumor morphology. Let (q_i, k_i) denote the training set data with the input features q_i, output stiffness k_i, i=1, …, n. The RBF kernel was chosen as:

$$K(q_i, \boldsymbol{q}) = e^{-\gamma \|q_i - \boldsymbol{q}\|^2} \quad (3)$$

where γ is the kernel parameter. The optimal coefficients such as the γ in Eq. (3) and the cost function parameter which determines the tradeoff between minimizing training errors and minimizing the model-complexity [14] were under grid searching and a hyperplane was properly found to fit the training set data.

III. Results and Discussions

A silicon phantom (18cm x 30cm) embedded 8 inclusions was designed as a breast tumor phantom for robot-assisted tumor detection experiment. These tumors were arranged as shown in Fig. 10. The robot moved the palpation probe along the designated path (indicate as the red lines) to scan the whole surface of the phantom.

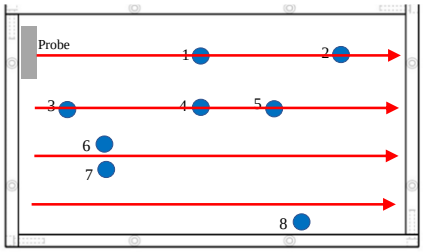

Fig. 10 The Phantom with Designated underlying Tumor and the Robot-held Probe Moving Path

At the same time, the computer will record the moving position of the probe and the contact forces. After processing the measured signal by eliminating the ground force of the soft tissue, the force data displayed as shown in Fig. 11. The threshold method was applied to find the force peak of the force data and identified peak number 1~8 and FP1~3.

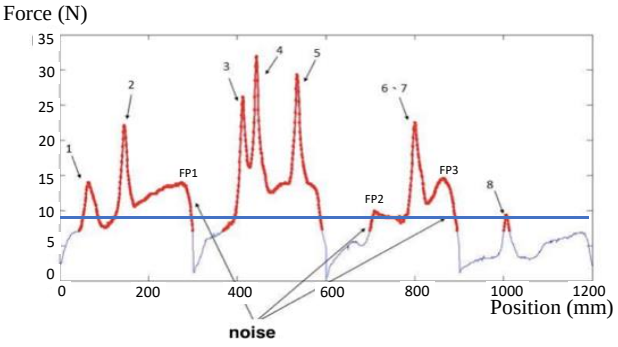

Fig. 11 Detection of Force Peaks

The force peaks may be also produced by fake noise, the slope property was then applied to screen out these false features. As shown in Fig. 12, tumor 1~8 was all displayed the pattern of increasing to positive value followed by decreasing to negative valley. Whereas the FP1~3 was not able to show the slope pattern and judged to be false features for tumor existence.

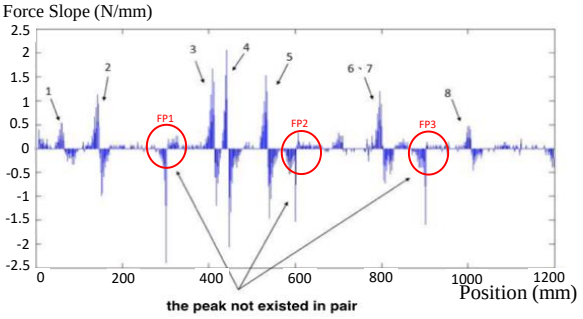

Fig. 12 Confirmation of the Slope Property of the Force Curve

Last to confirm the tumor existence was to check the shape similarity by calculating the correlation of the measured force curve with the nominal force curve as Fig. 8. As shown inTable 1, the correlation numerical for tumor 1~8 was more than 90%. The result (in Fig. 13) demonstrates that the robot-assisted palpation approach could reliably detect the tumor existence underneath soft tissue.

Table 1. Confirmation of the force shape correlation

Tumor Location	1	2	3	4	5	6,7	8
Shape Correlation (%)	91.8	99.2	99.1	96.1	98.6	93.6	91.0

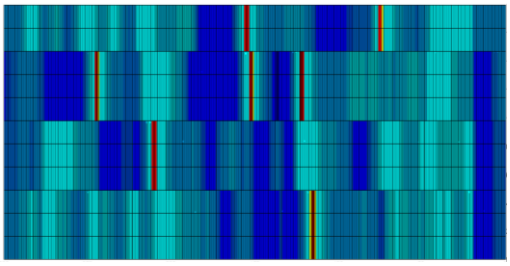

Fig. 13 The location of tumor existence by robot detection

It was also observed that the size of the probe affected the detection sensitivity of tumor existence. Large size of probe could detect the tumor existence, however can't distinguish whether it is single or multiple case. Although small size of probe could exhibit better sensitivity of tumor detection, the examination time could be obviously increased.

The other experiment is to verify the effectiveness of tumor stiffness prediction. In addition to the tumors with trained stiffness 5, 10, 15, tumors with two interpolated stiffness 7 and 12 were also under study. The results are shown in Table 2. As observed from the results, the predicted errors for tumor stiffness were 8% for the group with the same values of stiffness as the training data, and 15% for those with interpolated values of stiffness. The errors are acceptable for most of diagnostic cases, in which the stiffness information can assist the physician to differentiate the ambiguity of benignity and malignancy when single image modality is used. For example the ultrasound image features of fibroderoma and IDC are not easy to differentiate, but the tumor's stiffness are significantly different. Therefore such mechanics information becomes very useful.

Table 2. Tumor Stiffness Prediction of the Trained SVR Model

	RMSE (%)
Training Set	1
Testing Set with trained stiffness (5, 10, 15)	8
Testing Set with interpolated stiffness (7, 12)	15

IV. Conclusion and Future Work

A robot-assisted palpation system for breast tumor detection and further identification of the bimechanical property has been demonstrated. The robot-assisted palpation could carry out a stable palpation behavior and subsequently achieved accurate outcomes. The results showed that the tumors could be detected if the tumor sizes not less than 5mm, which indicates to be in early stage. Moreover, the system can also predict the stiffness of the tumor and offer the second opinion for the physician to diagnose its benignity or malignancy. The future work may extend the current method to deal with non-flatness effect of the breast using the compliance control of the robot system, and then towards clinical validation.

References

[1] W. S. Bernard, P. W. Christopher, World cancer report 2014. IARC (International Agency for Research on Cancer), Lyon, France, 2014.

[2] T. B. Bevers et. al, "Breast Cancer Screening and Diagnosis", Journal of the National Comprehensive Cancer Network, Vol. 7, No. 10, pp. 1060-1096, 2009.

[3] C. H. Lee et al, "Breast cancer screening with imaging: recommendations from the Society of Breast Imaging and the ACR on the use of mammography, breast MRI, breast ultrasound, and other technologies for the detection of clinically occult breast cancer", Journal of the American college of radiology, Vol. 7, No.1, pp. 18-27, 2010.

[4] A. Damera et al, "Diagnosis of axillary nodal metastases by ultra-sound-guided core biopsy in primary operable breast cancer", British journal of cancer Vol. 89, No.7, pp. 1310-1313, 2003.

[5] N. MA Krekel et al, "Intraoperative ultrasound guidance for palpable breast cancer excision (COBALT trial): a multicentre, ran-domised controlled trial", The lancet oncology, Vol. 14, No.1, pp. 48-54, 2013.

[6] A. Itoh, E. Ueno, E. Tohn, H., Kamma, H. Takahashi, T. Shiina, T. Matsumura, "Breast disease: clinical application of US elastography for diagnosis", Radiology, Vol. 239, No. 2, pp. 341-350, 2006.

[7] J. Ophir, B. Garra, F. Kallel, E. Konofagou, R. Righetti, T. Varghese, "Elastographic Imaging", Ultrasound in Med. & Biol, Vol. 26, No. 1, s23-s29., 2000.

[8] R. M. Delaine-Smith et al. "Experimental validation of a flat punch indentation methodology calibrated against unconfined com-pression tests for determination of soft tissue biomechanics", Journal of the mechanical behavior of biomedical materials, Vol. 60, pp. 401-415, 2016.

[9] J. T. Iivarinen, R. K. Korhonen, J. S. Jurvelin, "Experimental and numerical analysis of soft tissue stiffness measurement using manual indentation device–significance of indentation geometry and soft tissue thickness", Skin Research and Technology Vol. 20, No.3, pp. 347-354, 2014.

[10] P. L. Yen, H. C. Hsu, Y. C. Lin, "Robot-assisted identification of breast tumor biomechanics", IEEE International Conference on Industrial Technology (ICIT), pp. 1488-1490, 2016.

[11] T. Heimann, H. P. Meinzer, "Statistical shape models for 3D medical image segmentation: A review", Medical Image Analysis, Vol. 13, No. 4, pp. 543-563, 2009.

[12] P. L. Yen, R. H. Fan, D. Chen, Y. J. Chu, H. C. Hsu, Design and construction of 3D breast tumor phantoms for studying morphological effects on biomechanical properties, Int J CARS, Vol. 8 (Suppl 1): S284–S285, 2014.

[13] C. C. Chang, C. J. Lin, "LIBSVM: A library for support vector machines", ACM Trans. Intell. Syst. Technol., Vol. 2, No. 3, pp. 1-27, 2011.

[14] Ahmed G. Abo-Khalil and Dong-Choon Lee, "MPPT Control of Wind Generation Systems Based on EstimatedWind Speed Using SVR", IEEE Trans. on Industrial Electronics, Vol. 55, No. 3, pp. 1489-1450, 2008.